JACS
JOURNAL OF THE AMERICAN CHEMICAL SOCIETY

Article

pubs.acs.org/JACS

Modulating Semiconductor Surface Electronic Properties by Inorganic Peptide–Binders Sequence Design

Maayan Matmor and Nurit Ashkenasy*

Department of Materials Engineering and the Ilze Katz Institute for Nanoscale Science and Technology, Ben Gurion University of the Negev, Beer-Sheva, Israel

Supporting Information

ABSTRACT: The use of proteins and peptides as part of biosensors and electronic devices has been the focus of intense research in recent years. However, despite the fact that the interface between the bioorganic molecules and the inorganic matter plays a significant role in determining the properties of such devices, information on the electronic properties of such interfaces is sparse. In this work, we demonstrate that the identity and position of single amino acid in short inorganic binding protein-segments can significantly modulate the electronic properties of semiconductor surfaces on which they are bound. Specifically, we show that the introduction of tyrosine or tryptophan, both possessing an aromatic side chain which higher occupied molecular orbitals are positioned in proximity to the edge of GaAs valence band, to the sequence of a peptide that binds to GaAs (100) results in changes of both the electron affinity and surface potential of the semiconductor. These effects were found to be more pronounced than the effects induced by the same amino acids once bound on the surface in a head–tail configuration. Furthermore, the relative magnitude of each effect was found to depend on the position of the modification in the sequence. This sequence dependent behavior is induced both indirectly by changes in the peptide surface coverage, and directly, probably, due to changes in the orientation and proximity of the tyrosine/tryptophan side group with respect to the surface due to the preferred conformation the peptide adopts on the surface. These studies reveal that despite the use of short protein oligomers and aiming at a non-natural-electronic task, the well-known relations between the proteins' structure and function is preserved. Combining the ability to tune the electronic properties at the interface with the ability to direct the growth of inorganic materials makes peptides promising building blocks for the construction of novel hybrid electronic devices and biosensors.

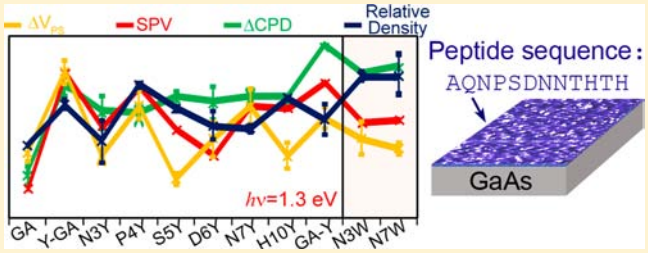

INTRODUCTION

The modularity in the design and synthesis of organic molecules has opened the way to use organic monolayer self-assembly to tailor the chemical and physical properties of inorganic surfaces.[1−3] In a common design, the headgroup of the molecules binds to the surface of the material while a functional group is coupled to the molecules' tail in order to modify the desired surface property. Such molecular monolayers have been proven to be a powerful tool for tailoring electronic properties of semiconductor surfaces in terms of both surface dipole[4−9] and surface potential (i.e., surface band bending).[7,10−15] These effects have been utilized for modulating the properties of nanodevices,[16] Schottky diodes,[17−20] and for the development of chemi- and bio- field-effect transistor (FET) sensors.[20−24] While the flexibility in the choice of the tail group of the molecules makes this approach quite modular, the magnitude of the effects is limited due to its distance from the surface and its confined orientation with respect to the surface. Furthermore, in many cases, especially concerning charge redistribution at the surface, the effects are dominated by the nature of the headgroup.[10,25−29]

The growing interest in the development of novel bioelectronic devices,[30−32] as well as different types of biosensors that rely on the transduction of biological signal to an electrical read-out,[21,33−35] stimulate the need to understand electronic interactions of proteins with inorganic interfaces.[36] This is of critical importance since these biomolecules do not adopt the common head–tail configuration; hence, the behavior of the interface cannot be clearly predicted. In particular, it is important to understand if and how the position of a functional group on the protein affects the interface electronic properties.

Protein immobilization on surfaces is usually achieved by the use of antibody–antigen interactions.[37,38] For direct binding chemical bonding through amino acid side chains, such as cysteine, lysine, or glutamic and aspartic acid, are commonly used.[32] In the natural system, on the contrary, the interface between bioorganic molecules and inorganic matter is typically comprised of multiple weak interactions. Such interfaces have been recently mimicked by the use of inorganic peptide binders

Received: August 7, 2012
Published: November 27, 2012

dx.doi.org/10.1021/ja3078494 | J. Am. Chem. Soc. 2012, 134, 20403–20411

(IPBs).[39] A large variety of IPBs with affinity to diverse materials including metals, insulators, semiconducting and magnetic materials, have been screened using combinatorial biological libraries,[40−43] demonstrating unprecedented design flexibility which is important for device engineering. Such IPBs have been used as templates for growth of inorganic nanoparticle films and nanostructures.[42,44−46] We have recently demonstrated that dual affinity IPBs can be used to pattern inorganic materials on predefined locations on a substrate by microcontact printing,[47] enabling the formation of multicomponent patterns of diverse materials on practically any substrate of choice. A pioneering demonstration for the use of IPBs to control electronic device performance was given by Dezieck et al.[48] They have controlled the threshold voltage of an organic FET in a range of 30 V by adjusting the dipole of an IPB layer deposited on the device gate by controlling the pH of the solution used for the IPBs deposition. Our own studies have indicated that, in addition to dipolar effects, charge transfer may also occur at the IPB−inorganic hybrid interface.[45] This is despite the fact that peptides seemingly bind to surfaces by weak interactions, which do not necessarily involve charge transfer processes. These studies, hence, indicate that it may be possible to use IPBs to tailor electronic properties at the interface with inorganic material. However, it is important to understand if, and to what extent, these processes could be affected by the peptide sequence since such sequence dependence may open a simple way to optimize these effects. In this work, we examine the influence of IPBs' binding on the electronic properties of semiconductor surfaces. Using a small library of IPBs that includes a series of peptides with point mutation of a "native" sequence,[39] in which natural amino acids tyrosine (Y) and tryptophan (W) were introduced at different locations along the sequence, we show that peptides can affect the surface electronic properties of GaAs both by dipolar and charge redistribution effects. Furthermore, we demonstrate the sensitivity of the electronic effects to both the position and the nature of functional groups on the peptide.

EXPERIMENTAL SECTION

Materials. Peptides with >95% purity, capped on both ends, were purchased from GL Biochem (China). Amino acids with purity of 98% and eutectic indium−gallium alloy 99.99% were purchased from Sigma Aldrich, Israel. HPLC grade acetonitrile, acetone, and ethanol (J. T. Baker) and triply distilled water (TDW, 18.2 MΩ, EASYpureRoDi, Thermo Scientific) were used for the preparation of the samples. NH_4OH (29%) was used in the cleaning etching process (J. T. Baker). Assembly experiments were done in Phosphate buffer saline (PBS, Biological Industries, Israel).

Samples Preparation. Samples (1 cm^2) were cut from Si doped (4.9×10^{16} cm^{-3}) GaAs (100) wafers (2.6×10^{-2} Ω·cm resistivity, Institute of Electronic Materials Technology, Poland). Samples were cleaned using heated sonication bath in ethanol/acetone 1:1 (v/v) ratio for 15 min, followed by 35 min UV/ozone treatment (Novascan Industries Ltd.). Samples were then etched in basic solution (NH_4OH/TDW 1:9, v/v) for 1 min, and rinsed in TDW for 1 min. Immediately after cleaning, the samples were transferred into a glovebox (O_2 < 0.1 ppm, H_2O < 1 ppm, MBRAUN, MB 20G) and were immersed in 1 mg/mL solution of the peptide in PBS (pH = 7.4). For amino acids assembly, the samples were immersed in 1 mM solution of the amino acids in acetonitrile. After overnight assembly time, the samples were thoroughly washed in TDW and dried in a vacuum chamber for 1 h.

Structural Characterizations. Peptide monolayers' thickness was measured by ellipsometry (SE800, Sentech Instruments GmbH, Germany) at a wavelength of 632 nm and angle of 70°. Measurements were conducted immediately after deposition in order to eliminate surface oxidation. Thickness values were calculated using a refractive index of 1.46 and averaged over three different samples. X-ray photoelectron spectroscopy (XPS) experiments were conducted using an ESCALAB 250 instrument equipped with an Al X-ray source and monochromator (Thermo Scientific, U.K.). Samples were transferred from the glovebox into the XPS vacuum chamber without exposure to air using a homemade introduction chamber. The obtained spectra were calibrated with respect to the C-1s binding energy (284.5 eV). The atomic percentage of nitrogen was evaluated from the ratio of the N-1s and Ga3d peak areas, with peak fitting obtained using the ThermoAdvantage software of the instrument with smart background subtraction. For accurate determination of the nitrogen peak area, a small satellite Auger peak of Ga at 390 eV, which slightly overlaps with the nitrogen peak, was removed from all spectra by estimation of its area from the bare GaAs sample. Values present average of three different samples.

Electrical Characterizations. Electrical characterizations were obtained in a contactless manner using the Kelvin probe technique (Kelvin probe S, Besocke, Germany), which measures the contact potential difference (CPD) between the sample and a reference gold electrode.[49] Fresh samples were mounted in a dark Faraday cage operating under a nitrogen flow (15% humidity) in order to minimize effects of oxidation and artifacts obtained due to changes in the humidity. Contact to a grounded sample holder was achieved by scratching the back of the sample and introduction of a layer of eutectic InGa solution. Dark CPD values, which correspond to the difference in the work function of the sample and the reference gold electrode (ϕ_{Au} = 5 eV), were recorded and averaged for at least five different samples for each peptide library member. Surface photovoltage (SPV) spectra were recorded by illuminating the sample at a wavelength range of 1600−600 nm using the output of a xenon−mercury light source transferred through a double monochromator (MS 257, Newport, USA) and a long pass filter (in order to eliminate second order reflections). Spectra were collected, using Tracq 32 software (Newport, USA) for a freshly prepared set of samples of hybrids of all the library members in one day. Representative results of one of the batches are presented. While some variations in the magnitude of the signal were observed for other batches of samples, the relative signal magnitudes showed the same typical behavior for at least 80% of the examined batches.

band bending (V_{BB}) measurements were conducted by illuminating the samples with a 532 nm diode laser (80 mW, Brighten optics Ltd., Canada) using the same Kelvin probe configuration. The beam was collimated to a diameter of 1.5 cm on the sample. The intensity of the laser was controlled using a circular variable neutral density filter (Newport) until a saturation of the signal was obtained. To exclude photochemical effects, it was verified that the samples regained their dark (equilibrium) CPD value after the laser light was switched off. Presented V_{BB} values are the average of 3−5 different samples.

RESULTS AND DISCUSSION

The main hypothesis in this research was that peptide monolayer binding may affect the electronic properties of semiconductor surfaces due to interactions with the side chains of the peptide. We postulated that such effects may depend on the nature of the side chains and, furthermore, on the orientation and proximity of such side chains with respect to the surface, and hence may result in larger effects than these induced by head−tail monolayer configuration. We, therefore, anticipated that the surface electronic response should be different for isolated amino acid bound to the surface through its carboxylic group than for the same amino acid in the context of a peptide binding segment. Furthermore, if the peptide adopts preferred conformation on the surface, the response should depend on the position of functional amino acids in the sequence. These hypotheses were studied using GaAs, a

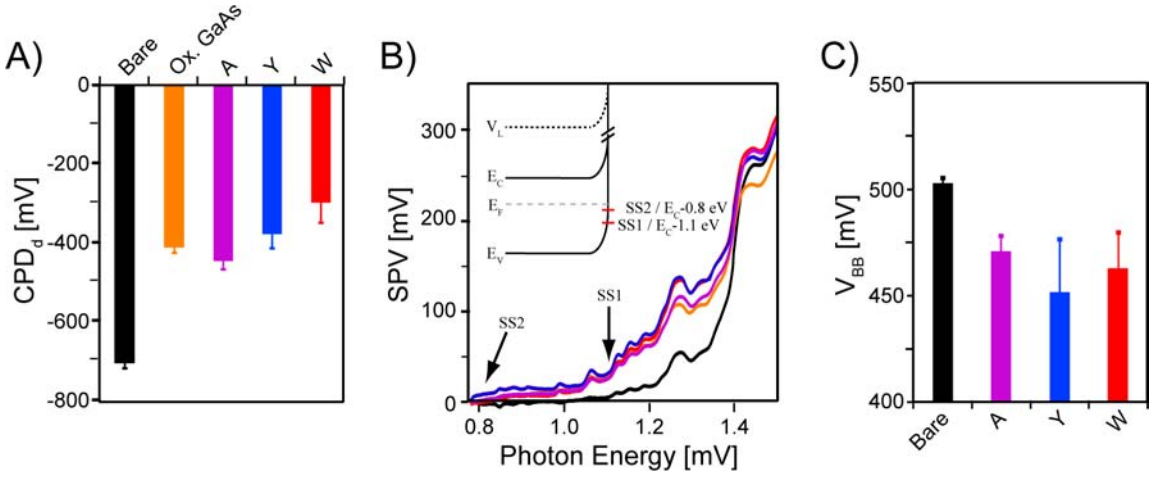

Figure 1. Electrical characteristics of bare GaAs, and GaAs functionalized with alanine, tyrosine and tryptophan amino acid monolayers. (A) Dark CPD of the different samples. (B) SPV of the different samples. Color scheme is the same as in A). SS1 and SS2 mark the onset of the SPV slope due to electron transitions from surface states SS1 and SS2 (marked in the inset) to the conduction band, respectively. The small peaks in the SPV spectra are due to features in the spectrum of the Xenon (Mercury) light source used for the measurements (marked by * in Figure S2). The inset represents the surface energy bands diagram obtained from the analysis of the SPV spectra. (C) V_{BB} of the different samples. V_{BB} was obtained using a 80 mW diode laser (λ = 532 nm). Verification of photosaturation conditions was obtained by measuring the signal as function of laser intensity (Figure S3).

common semiconductor, for which an IPB has been identified using a phage display library screening methodology.[39]

The electronic effects, which can be induced by binding of such peptides on the semiconductor surface, include changing the semiconductor electron affinity by dipolar effects and altering the surface potential by charge redistribution, both of these effects modulating the semiconductor work function, Φ_S.[49] We have, therefore, used the Kelvin probe technique to monitor the work function of the samples by means of the contact potential difference (CPD), which is expressed as

$$e(\mathrm{CPD}) = \Phi_s - \Phi_{ref} \quad (1)$$

where e is the electron charge, and Φ_{ref} is the work function of the reference (gold) Kelvin probe (Φ_{ref} ~5 eV). Since illumination of the sample can result in changes in the surface band bending by means of a surface photovoltage (SPV) due to charge excitation and redistribution across the surface space charge region, recording the CPD both in dark, CPD_d and under illumination, CPD_l, provided the SPV as:[15]

$$\mathrm{SPV} = \mathrm{CPD_d} - \mathrm{CPD_l} \quad (2)$$

Hence, monitoring the SPV at varying wavelengths provided information on changes in surface states occupation. Further insight into charge redistribution due to amino acid monolayers adsorption was obtained by monitoring changes in the surface band bending potential, V_{BB}. Such measurements were carried out by measuring the SPV response due to exposure to a large flux of photons with super bandgap energies. For such conditions, the energy bands of the semiconductor flatten; hence, the SPV value corresponds to V_{BB}.[50] We note that, while the validity of these measurements in obtaining the true band banding of semiconductors has been disputed,[50,51] the deviations from the true band bending, which are related to bulk effects, should be similar for all the samples, and thus, changes in V_{BB} between different samples indeed reflect changes in the surface band-bending. Furthermore, since CPD_d is composed of V_{BB} and dipolar contributions, comparing the two first quantities for each hybrid enabled monitoring changes in the dipolar contribution.

In the following, we will first use CPD measurements to monitor electronic effects induced by binding three different amino acids, tyrosine, tryptophan, and alanine, with head–tail configuration on the surface. We then describe the design of a small library of GaAs IPBs that includes tyrosine and tryptophan modifications at different positions along the "native" IPB sequence. After characterization of the effects of such modifications on the surface coverage of the IPBs on GaAs, we provide detailed studies of the electronic effects induced by the library members on GaAs surface electronic properties, emphasizing on amino acid position dependence.

Electronic Effects of Individual Amino Acids. The effects of three amino acids, tyrosine, tryptophan, and alanine, on the electronic properties of GaAs (100) were studied. Tyrosine and tryptophan were chosen since their highest occupied molecular orbital (HOMO) was estimated to overlap, or be slightly above the valence band of GaAs (Figure S1),[52,53] suggesting possible electronic interactions between them. Alanine was chosen as a reference to study the effect of the carboxylic headgroup on the electronic properties. The assembly of these amino acids on GaAs (100) through their carboxylic group, forming a common head–tail monolayer configuration, was confirmed by ellipsometry and contact angle measurements (data not shown). An increase in the CPD (and thus in the work function) was observed in all three cases (Figure 1A). The 250 mV increase in the CPD of the GaAs surface once functionalized with alanine can be attributed to the contribution of the bonds of the carboxylic headgroup with the surface or to the polar amine group. Further increase in the CPD, obtained once tyrosine and tryptophan have been bound to the surface suggests that the aromatic side groups of these amino acids affect the electronic properties of the surface, with tryptophan showing a more pronounced effect than tyrosine. We note that the CPD of GaAs sample which was subjected to the same preparation conditions, but without the oxide removal and peptide assembly steps, was larger than that of the bare clean surface but smaller than that of surfaces covered with tyrosine and tryptophan monolayers (Figure 1A), indicating

dx.doi.org/10.1021/ja3078494 | J. Am. Chem. Soc. 2012, 134, 20403–20411

that the changes observed due to amino acids assembly cannot be attributed solely to surface oxidation effects.

Changes in the CPD can be attributed both to monolayer induced dipolar effects and to charge redistribution. Hence, we have used SPV measurements to monitor charge redistribution effects separately. SPV spectra indicated changes in the occupation of surface states due to monolayer adsorption (Figure 1B). In such spectra, a slope onset corresponds to SPV induced by electron transition between energy bands, which energy difference can be deduced by the onset point.[49] Furthermore, the slope inclination direction and angle can be used to identify which electronic levels are involved in the transition and the density of states. Accordingly, the substantial increase in the SPV at 1.4 eV, observed for all the samples (Figure 1B), corresponds to super bandgap photon absorption, accompanied by a typical flattening of the energy bands. The emergence of a sub-bandgap SPV response at 1.1 eV (marked as SS1 in Figures 1B and S2) with a positive slope for all the samples, indicates photoinduced electron transition from a surface state located 1.1 eV below the conduction band (inset of Figure 1B) to the conduction band. A pronounced enhancement of this sub-bandgap response was observed for samples covered with the amino acids, indicated by an increase in the tilt of the slope above 1.1 eV. Such an enhancement can be attributed to an increase either in the density of electrons at the surface state, or the band-bending, due to amino acids' adsorption. Since, as will be shown below, the band-bending decreases due to amino acid assembly, we conclude that the first mechanism is the dominant one. Furthermore, a new sub bandgap response appeared in the spectra with an onset at ~0.8 eV (marked SS2 in Figures 1B and S2), again with a positive slope, indicating the formation or promoted occupation of an additional surface state, located 0.8 eV below the conduction band (inset of Figure 1B). The changes in the density of electrons in surface-states can be related to the formation of bonds between the carboxylic headgroup and the surface. The sub-bandgap response was observed to be slightly enhanced for surfaces functionalized with tyrosine and tryptophan compared to surfaces functionalized with alanine, suggesting that the aromatic tail group of these amino acids slightly contributes to the surface states electron density, as anticipated from the molecule–GaAs band alignment (Figure S1). It should be noted that the SPV response of the oxidized sample was very similar to the one obtained for the surface functionalized with alanine, again indicating that the response to functionalization with tyrosine and tryptophan cannot be solely attributed to sample oxidation. A decrease in V_{BB} was observed for surfaces on which amino acids were adsorbed (Figure 1C). This decrease, which inevitably is accompanied by decreasing the distance between the Fermi level and the conduction band, confirms that the large sub-bandgap response is due to an increase in electron density in surface states SS1 and SS2 that is induced by amino acid adsorption.

A decrease in the surface band-bending for an n-type semiconductor should result in a decrease in the work function and thus in the CPD, in contrary to the trends observed for the amino acid functionalized surfaces (Figure 1A). This behavior indicates a significant dipole contribution of the molecules, which increases the semiconductor surface electron affinity.[5] This dipole may originate from the polar amine group of the amino acids. However, the differences in the CPD between the samples covered with different amino acids clearly demonstrate a dipolar contribution of the amino acids side chains. This contribution seems to be larger for samples covered with tyrosine and tryptophan, with the largest dipole effect being detected for the later.

Overall, it can be concluded that for amino acid monolayers the carboxylic headgroup dominates the induced electronic effects; both increasing the semiconductor effective affinity, and reducing the surface band bending. Furthermore, while a minor contribution of the amino acid side chains is observed, the side chains mainly affect the surface electron affinity. While these studies may suggest that peptide side chains may induce only moderate effects on GaAs surface electronic properties, the actual effects may be enhanced in the context of a peptide due to larger proximity, and changes in the orientation of the side chains with respect to the surface. Furthermore, the elimination of carboxylic binding groups can be used to highlight the sole effects of peptide side chains. These behaviors will be highlighted in the next section.

IPBs Library Design. To study the electronic effects induced by tyrosine and tryptophan in the context of a peptide, we have chosen to use a sequence of an IPB that binds to GaAs (100) surface (**GA**, Table 1) that has been identified using a phage display library screening methodology.[39] This sequence was shown to retain its binding affinity and selectivity in the context of an isolated synthetic peptide.[54,55] On the basis of the electronic effects of amino acids binding, we have postulated that the incorporation of tyrosine or tryptophan, which are not included in the "native" peptide, may enhance the electronic interactions. Furthermore, it has been suggested that if the peptide adopts defined conformation on the surface, altering the position of the modification in the sequence would alter the proximity and orientation of its side chain with respect to the surface and its environment, and may thus control the magnitude of the effects. Hence, a small library of peptides, which contained modifications of **GA** with tyrosine and tryptophan at different positions along the sequence, was constructed (Table 1).

Table 1. List of IPB Sequences Used in This Work

Peptide Name[a]	Peptide Sequence[b,c]
GA[d]	AQNPSDNNTHTH
Y-GA	YAQNPSDNNTHTH
N3Y	AQYPSDNNTHTH
P4Y	AQNYSDNNTHTH
S5Y	AQNPYDNNTHTH
D6Y	AQNPSYNNTHTH
N7Y	AQNPSDYNTHTH
H10Y	AQNPSDNNTYTH
GA-Y	AQNPSDNNTHTHY
N3W	AQWPSDNNTHTH
N7W	AQNPSDWNTHTH

[a]Peptide mutations were named K#M, where K represents the replaced amino acid, # is its position along the peptide sequence (from the N-terminus), and M is the incorporated amino acid. GA-Y and Y-GA represents tyrosine addition mutations at the C- and N-termini, respectively. [b]Amino acids are given by their single letter abbreviations. [c]Amino acid mutation position is highlighted in bold blue/red color for tyrosine/tryptophan. [d]GA is the "native" peptide.[39]

dx.doi.org/10.1021/ja3078494 | J. Am. Chem. Soc. 2012, 134, 20403–20411

The sequences were designed such that the basic sequence was mutated near possible binding sites to the GaAs surface.[39,54,56] Thus, tyrosine was used to replace amino acids at positions 3, 6, and 7 near glutamine or asparagine that can form Lewis pair with the substrate. Additionally, since threonine and serine were found to be abounded amino acids in sequences screened for GaAs binding, positions 4, 6, and 10 were also mutated by tyrosine. We note that in peptides **N3Y** and **N7Y**, asparagine, which appears multiple times in the peptide sequence, was mutated, allowing examination of its importance for the peptide binding. Two additional tyrosine modifications at the two ends of the peptide were also tested. It was postulated that for these mutations minimal distortion of peptide structure will be obtained, maintaining the conformation of the "native" peptide. Finally, in order to test the importance of the chemical nature of the side group, we have mutated positions 3 and 7 which were found to impose weak/large electronic effects, respectively, with tryptophan as well. Peptides were capped on both ends to eliminate possible effects of their charge on the binding, and on the resulting electronic properties.

Peptides' Assembly. Peptide assembly was confirmed by the appearance of a nitrogen 1s peak in the XPS spectra of the GaAs surface, which did not appear for the bare surface. Relative surface coverage of the different peptides was estimated by the ratio of the N-1s and Ga3d peak areas (Figure 2). The results indicate that the incorporation of

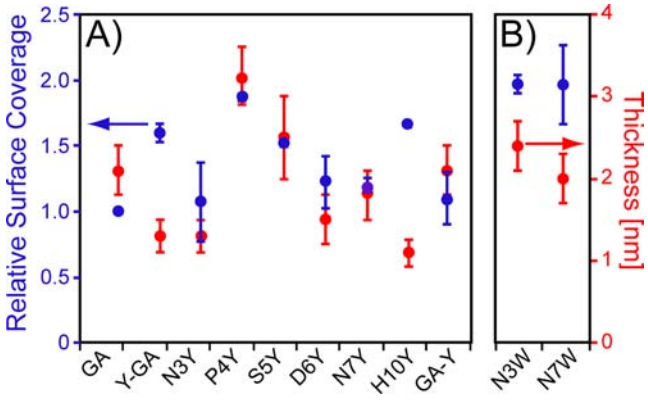

Figure 2. IPBs surface coverage and effective thickness for tyrosine (A) and tryptophan (B) mutations of GA. Surface coverage (blue) was calculated from XPS measurements (details are given in the Experimental Section). Values were normalized with respect to the coverage of the GA–GaAs hybrid. Effective peptide layer thicknesses (red) were obtained from ellipsometry measurements, taking into account a refractive index of 1.46. Presented values are average of measurements of three samples with the errors calculated by the standard deviation.

tyrosine at different locations maintains or enhances the binding affinity of the IPB. The observed increase in surface coverage indicates that the introduction of tyrosine enhances the binding interactions of the peptide with the surface. This could be as a result of direct interactions between the phenol side group and the surface, as will be shown below. The introduction of tryptophan instead of tyrosine resulted in larger surface coverage (Figure 2B). This is in line with the observation by Peelle et al., who found that tryptophan possess binding affinity to some semiconductors.[57] Such changes in the surface coverage can, in addition, suggest changes in the conformation of the peptide on the surface. For example, the 2-fold increase in surface coverage, which was obtained upon assembly of **P4Y** may be attributed to the elimination of the proline from the peptide sequence, which makes the peptide more flexible to adopt an optimal conformation with respect to the surface.

Further verification of peptide binding was obtained by ellipsometry measurements (Figure 2). The resulting peptide layer thicknesses were in the range of 1–3 nm, values that are much smaller than the extended length of the peptides (~4 nm). These values suggest the formation of a monolayer on the surface with possibly multiple binding sites to the surface. The thickness variation trends are in general agreement with the surface coverage trends observed by XPS, indicating that these variations reflect changes in the surface coverage and not in the effective peptide layer thickness. It is thus not possible to refer these variations to changes in the conformation of the peptides. However, in some cases, for example for **Y-GA**, **N3Y**, and **H10Y** hybrids, the effective thickness was lower than expected, suggesting that for these mutations the peptide has adopted a flatter conformation.

Electronic Properties of IPB/GaAs Hybrids. An increase of 100 meV in the CPD of GaAs was detected after the assembly of **GA** on the surface (Figure 3A), smaller than the effect induced by amino acid bound in head–tail configuration. This slight increase in the CPD, and the absence of change in the V_{BB} and sub-bandgap responses (Figures 3B and 4A, respectively), indicate that **GA** mostly affects the surface electronic properties by a dipole contribution to the work function, probably due to the net dipole of the peptide once

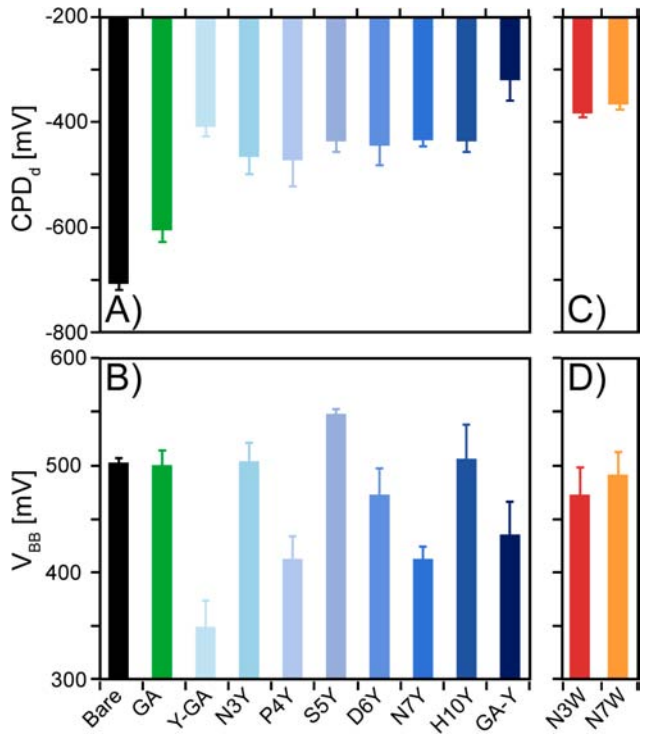

Figure 3. Electronic properties of GaAs functionalized with modified GA monolayers. (A) Dark CPD and (B) V_{BB} of GaAs functionalized with tyrosine modifications of GA. (C) Dark CPD and (D) V_{BB} of GaAs functionalized with tryptophan modifications of GA. Verification of photosaturation conditions was obtained by measuring the signal as function of laser intensity (Figure S3).

dx.doi.org/10.1021/ja3078494 | J. Am. Chem. Soc. 2012, 134, 20403–20411

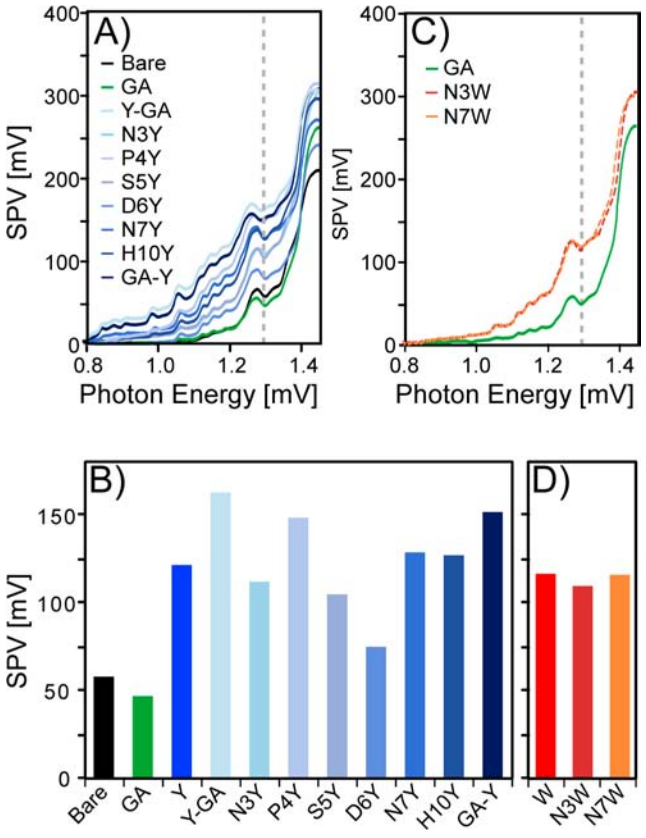

Figure 4. SPV spectra of GaAs surfaces functionalized with IPBs. (A) SPV spectra and (B) SPV at $h\nu$ = 1.3 eV (marked by dashed line in A) for GaAs functionalized with tyrosine modifications of GA. Color codes are the same in both panels. (C) SPV spectra and (D) SPV at $h\nu$ = 1.3 eV of GaAs functionalized with tryptophan modifications of GA. Color codes are the same in both panels.

absorbed on the surface. In addition, the lack of changes in the SPV and V_{BB} responses of the GaAs surface indicate weak interactions of the carboxylic group of the aspartic acid at position 6 with the surface. This may suggest that it does not play a significant role in the binding of **GA** to the surface. Indeed its removal in mutation **D6Y** did not affect the binding affinity to the surface drastically (Figure 2).

Modifying **GA** by the introduction of tyrosine strongly affected the electronic behavior of the peptide−GaAs hybrid interfaces. A significant increase in the CPD was observed for all the hybrids (Figure 3A). These effects were found to be much more pronounced than the effects induced by the binding of the "native" peptide, **GA**, hence indicating a large effect of the phenol side chain of tyrosine. In fact, the effect of the phenol group seems to be significantly larger in the context of the peptide than for its introduction in the context of isolated amino acids. Furthermore, taking into account the fact that the density of phenol groups on the surface is probably smaller for the peptides, the larger response shows a more significant response at the molecular level. The effect of tyrosine on the interface electronic properties was further revealed by observing the changes in V_{BB} upon peptide binding (Figure 3B). No change in V_{BB} was observed for surface functionalized with **GA**, indicating week electronic interactions. Similar behavior was observed for some of the peptide mutations, that is, for **N3Y**, **S5Y**, **D6Y**, and **H10Y**, suggesting that for these mutations the electronic interactions of the phenol group with the surface are week. In other cases, that is, for **Y-GA** **P4Y** and **N7Y**, the assembly resulted in a decrease in V_{BB}, probably indicating a reduction in the band-bending of GaAs at the hybrid interface (Figure 3B). These results indicate direct electronic interaction between the phenol side group of tyrosine and the surface. It should be noted that the suggested charge transfer interactions may account for the larger surface coverage obtained for **Y-GA** and **P4Y**. However, assembly of **N7Y** was not accompanied by an increase in the surface coverage, suggesting that the charge redistribution effect is more effective at the molecular level for this specific modification. Despite the fact that V_{BB} either decreased or remained intact, the CPD increased drastically in all cases, similar to the behavior observed for surfaces functionalized by isolated amino acids. This suggests that in addition to affecting the band bending, the phenol group introduces a pronounced positive dipole contribution in all cases.

Charge redistribution effects were further highlighted by the sub-bandgap SPV signal of the hybrid structures (Figure 4). In all cases, except for the case of the "native" peptide, the adsorption of the IPB on the surface has resulted in the appearance of a pronounced sub-bandgap response, indicating a direct effect of the phenol group on the surface states density or their occupation, further confirming direct electronic interactions between the phenol group and the surface. The energetic positions of the observed surface states were similar to these observed for the isolated amino acid hybrid interfaces. We note that it is hard to distinguish, at this point, whether charge redistribution occurred between the surface and the bulk of GaAs, or (and) between the GaAs and the peptide.

Differences in the magnitude of the electronic responses, as well as the surface coverage, were observed for the different peptide mutations (Figures 2−4 and Figure S4). These effects are summarized in Figure 5, clearly showing that each of the

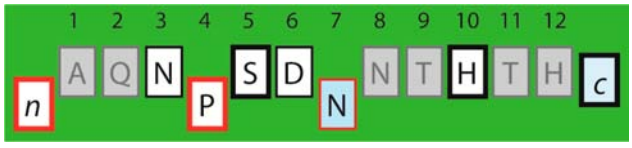

Figure 5. Depiction of the interactions of different tyrosine modifications of GA with the surface of GaAs (100). Each square represents a position on the peptide with the letters designating the sequence of the "native" peptide using amino acids' single letter abbreviation. The codes used to represent the strength of interactions for the different mutations are the following: thick borders represent large electron surface density; red borders and down shift represent large electron charge redistribution at the GaAs surface, with the magnitude of the shift representing relative strength of the interaction; light blue background represents strong dipolar effect. Positions marked in gray were not tested (see design details above).

different effects depends on the position of the tyrosine mutation in the sequence. In some of the cases, especially when the tyrosine was incorporated toward the N-terminus of the peptide, the changes in the electronic properties could be correlated with changes in the peptide surface density; that is, the larger the surface density, the larger the change in the CPD, SPV, and V_{BB}. However, this behavior cannot be simply explained by the dependence of the electronic properties on the phenol group density on the surface. That is, since, as suggested above, the induced reduction in surface band bending and positive dipolar contribution observed upon introduction of the

dx.doi.org/10.1021/ja3078494 | J. Am. Chem. Soc. 2012, 134, 20403−20411

phenol should affect oppositely the work function, hence, increasing both should result in a moderate change in the CPD. This is indeed the case for **P4Y** (Figure 3A and Figure S4). However, the large change in V_{BB}, sub-bandgap SPV and CPD observed upon assembly of **Y-GA** indicates strong electronic interactions accompanied by comparably large dipole effect. Furthermore, the incorporation of tyrosine at the C-terminus has a minute effect on the peptide surface coverage, but results in a large increase in the CPD and sub-bandgap SPV, accompanied by a moderate decrease in the band bending. The observed dependence of the electronic properties of the hybrids' interface on the position of tyrosine in the peptide sequence indicates that, in addition to the density of the phenol group on the surface, other parameters also affect the magnitude of the induced effects. These may include the proximity and the orientation of the phenol groups with respect to the surface and the dielectric environment, all of which are controlled by the preferred conformation the peptides adopt on the surface. An additional example for this complex dependence of the electronic properties on the location of the tyrosine modification in the sequence can be observed when looking at IPBs with tyrosine modifications at positions 4−7. Incorporating the tyrosine on positions 4, 5, and 6 results in gradually decrease in the surface coverage of the peptides and in the SPV while the CPD remains constant. V_{BB}, on the other hand, shows an unexpected decrease for the GaAs-S5Y hybrid (indicating an increase in the band bending), which is not observed in any other case. For **N7Y** functionalized surfaces, both significant decrease in V_{BB} and increase in the CPD are observed, suggesting both effective charge redistribution and large dipole contribution to the work function accompanied by no significant change in the peptide surface coverage with respect to the native peptide for this specific mutation. Finally, an exceptional behavior is observed for surface functionalized with **H10Y**. In this case, no significant change in the band bending is observed (Figure 3B), while a large sub-bandgap SPV response is induced. This behavior may suggest a unique role for tyrosine when inserted in this position, which results in changes in the surface recombination velocity. Alternatively, it may be attributed to electronic interactions of histidine with surface atoms for the "native" peptide due to its metal chelating character, which are eliminated once it is removed from the surface.

Our results show that the surface electronic characteristics of the semiconductor depend on the structure of peptides adsorbed on the surface. Unfortunately, the conformation of the peptide on the surface, which could be different for each of the mutations used, is hard to predict and monitor.[58] Furthermore, such small peptides are expected to be less structured, and thus, it is possible that the peptides adopt several preferred conformations on the surface. In addition, nonspecific adsorption may also occur. Hence, it is hard to directly correlate between peptide structure and the electronic behavior. Nevertheless, some of the observed electronic behaviors can be related to structural parameters. The interactions of tyrosine with the surface, which are demonstrated in this work, probably affect the conformation of the peptide. However, it can be anticipated that the conformation attained is restricted by the peptide sequence and the preferred conformation of the "native" peptide. For example, introduction of tyrosine at position 5 in **S5Y** results in week electronic interactions despite the large surface density. This can be explained by rigidity of the peptide chain around the proline at position 4, which restricts the flexibility of the phenol side chain to adopt a preferred orientation with respect to the surface. This rigidity can further explain the low surface density and small electronic effects upon the introduction of tyrosine at position 3 in **N3Y**. Additional sequence dependent response can be inferred by the differences in the electronic response for hybrids which includes tyrosine at the edges of the peptide. As suggested above, the use of an IPB in which the tyrosine is coupled at the N-terminus results in larger surface electronic interactions than for hybrids with IPB in which the tyrosine is attached at the C-terminus. This could be due to the presence of alanine at the N-terminus. Alanine does not interact by itself with the surface; hence, it allows rearrangement of the peptide on the surface upon the introduction of tyrosine to maximize the interactions of the phenol group with the surface. The THTH sequence at the C-terminus, which is considered to be a binding site of the peptide with the surface, probably adopts a more rigid structure with respect to the GaAs surface which restricts the ability of the peptide to deform and thus induces smaller electronic interactions (yet larger dipole effect). It is important to note that such changes in the conformation of the IPBs may also explain the changes observed in surface coverage, which by themselves also affect the electronic behavior, as demonstrated above for GaAs-P4Y hybrids.

As a final point, the effects of introduction of mutations incorporating tryptophan to the surface were tested. In similar fashion to the introduction of tyrosine, the introduction of tryptophan to the IPBs resulted in an increase in the CPD of the GaAs surface upon binding (Figure 3C). The magnitude of the change followed the same trends as for tyrosine mutations, that is, $\Delta CPD_{Trp} > \Delta CPD_{N7W} > \Delta CPD_{N3W}$, with the overall changes larger than when using the corresponding tyrosine analogs (Figure 3A). V_{BB}, on the other hand, was found to be similar in both cases (Figure 3B,D); hence, it cannot explain the CPD behavior. Furthermore, the changes induced in the sub-bandgap response were not significantly different (Figure 4); modification at the N3 position resulted in a similar response in both cases, whereas for the seventh position, functionalization with the tryptophan modified peptide resulted in smaller sub-bandgap response than for the tyrosine analog. These observations suggest that functionalization of the surface with tryptophan modifications of **GA** results in similar charge redistribution at the surface as for the tyrosine analogs. In fact, taking into account the larger surface density obtained for tryptophan analogues, the single molecule effect seems to be smaller in this case. In addition, as for the isolated amino acid case, tryptophan modifications of **GA** induce larger dipole effects, which increase the CPD (and work function) of the GaAs surface. It could be speculated that stronger dipole−dipole interactions result in larger affinity of the tryptophan−**GA** modifications to the surface and thus are responsible for the larger surface coverage. These results indicate that the specific choice of amino acid and its position in the peptide sequence can be used to dominantly modulate a specific property of the surface. Importantly, non-natural amino acids can also be used to further modify the interface by the introduction of light sensitizing or biorecognition side chains, paving the way to engineer novel devices based on such peptides.

■ CONCLUSIONS

We have demonstrated that the assembly of IPBs on semiconductor surfaces modulates the surface electronic properties both in terms of the electron affinity and the surface

potential in a manner that depends on the sequence that is used. Specifically, we have found that a commonly used GaAs IPB has a minor effect on the surface electronic properties in its "native" form. However, the introduction of tyrosine or tryptophan to the sequence results in pronounced dipolar and charge redistribution effects at the interface. The magnitude of each of these effects was found to depend on the position of the modification in the peptide sequence due to conformational changes that affect the IPB surface coverage and/or the proximity and orientation of the phenol/indole side chains of tyrosine/tryptophan with respect to the surface. Moreover, we have found that the incorporation of tryptophan increases the dipolar effect with respect to modification of the peptide with tyrosine on the same location. Further studies are required in order to understand the exact mechanisms by which sequence and conformation affect the electronic properties.

Our results clearly show that the unique structure−function relations of natural proteins can be preserved in unnatural environment. For electronic applications, the large interface formed between the biomolecules and the surface increases the magnitude of effects induced by functional groups on the biomolecules, resulting in effects that are larger than these imposed by the same functional groups attached in a common head−tail configuration. While general rules for tailoring the interface electronic properties by peptide design have not yet been provided, we show that if the functional amino acids have the flexibility to adopt a preferred orientation, the effects are enhanced. Furthermore, the ability to optimize the nature and position of a functional side group in proteins and peptides can be used to control independently the different electronic properties of their interface with inorganic materials. The introduction of other amino acids, including non-natural ones, may extent the magnitude of the effects and can be used for the introduction of additional functionalities, such as photosensitization. Hence, the interface of IPBs, or other protein and peptide architectures can be tailored to control the performance of hybrid bioelectronics and biosensing devices.

■ ASSOCIATED CONTENT

Supporting Information

Electronic energy levels scheme of the semiconductor and the corresponding functional group, SPV spectra with detailed analysis, super bandgap SPV as function of laser intensity, graphs showing the dependence of the relative density, CPD and V_{BB} change, and sub-bandgap SPV on the peptide modification site. This material is available free of charge via the Internet at http://pubs.acs.org.

■ AUTHOR INFORMATION

Corresponding Author

nurita@bgu.ac.il.

Notes

The authors declare no competing financial interest.

■ ACKNOWLEDGMENTS

This research was supported by a grant from the Israel Science Foundation (1293/08), and the Edmond J. Safra Foundation through the Biopolymers Center. The authors thank Dr. N. Frumin for performing the XPS experiments, and Mr. J. Jopp for the aid in ellipsometry measurements. M.M. is a recipient of a Kreitman school fellowship for doctoral research, and of the Israel Ministry of Science and Technology 2012 fellowship for the Advances of women in science.

■ REFERENCES

(1) Whitesides, G. M.; Kriebel, J. K.; Love, J. C. *Sci. Prog.* **2005**, *88*, 17.
(2) Bain, C. D.; Whitesides, G. M. *Angew. Chem.* **1989**, *101*, 522.
(3) Onclin, S.; Ravoo, B. J.; Reinhoudt, D. N. *Angew. Chem., Int. Ed.* **2005**, *44*, 6282.
(4) Vilan, A.; Cahen, D. *Trends Biotechnol.* **2002**, *20*, 22.
(5) Ashkenasy, G.; Cahen, D.; Cohen, R.; Shanzer, A.; Vilan, A. *Acc. Chem. Res.* **2002**, *35*, 121.
(6) Cahen, D.; Kahn, A.; Umbach, E. *Mater. Today* **2005**, *8*, 32.
(7) Vilan, A.; Yaffe, O.; Biller, A.; Salomon, A.; Kahn, A.; Cahen, D. *Adv. Mater.* **2010**, *22*, 140.
(8) Natan, A.; Kronik, L.; Haick, H.; Tung, R. T. *Adv. Mater.* **2007**, *19*, 4103.
(9) Heimel, G.; Romaner, L.; Zojer, E.; Bredas, J.-L. *Acc. Chem. Res.* **2008**, *41*, 721.
(10) Cohen, R.; Kronik, L.; Shanzer, A.; Cahen, D.; Liu, A.; Rosenwaks, Y.; Lorenz, J. K.; Ellis, A. B. *J. Am. Chem. Soc.* **1999**, *121*, 10545.
(11) Dorsten, J. F.; Maslar, J. E.; Bohn, P. W. *Appl. Phys. Lett.* **1995**, *66*, 1755.
(12) Rothschild, A.; Komem, Y.; Ashkenasy, N. *J .Appl. Phys.* **2002**, *92*, 7090.
(13) Hunger, R.; Jaegermann, W.; Merson, A.; Shapira, Y.; Pettenkofer, C.; Rappich, J. *J. Phys. Chem. B* **2006**, *110*, 15432.
(14) Hartig, P.; Rappich, J.; Dittrich, T. *Appl. Phys. Lett.* **2002**, *80*, 67.
(15) Zhang, Z.; Yates, J. T. *Chem. Rev.* **2012**, *112*, 5520.
(16) Naaman, R. *Phys. Chem. Chem. Phys.* **2011**, *13*, 13153.
(17) Slawomir, B.; William, R. S.; Mats, F. *Adv. Mater.* **2009**, *21*, 1450.
(18) Ishii, H.; Sugiyama, K.; Ito, E.; Seki, K. *Adv. Mater.* **1999**, *11*, 605.
(19) Vilan, A.; Shanzer, A.; Cahen, D. *Nature* **2000**, *404*, 166.
(20) Chen, K.-S.; McGill, S. A.; Xiong, P. *Appl. Phys. Lett.* **2011**, *98*, 123110.
(21) Khamaisi, B.; Vaknin, O.; Shaya, O.; Ashkenasy, N. *ACS Nano* **2010**, *4*, 4601.
(22) Mafé, S.; Manzanares, J. A.; Reiss, H. *J .Appl. Phys.* **2011**, *109*, 044302.
(23) Goykhman, I.; Korbakov, N.; Bartic, C.; Borghs, G.; Spira, M. E.; Shappir, J.; Yitzchaik, S. *J. Am. Chem. Soc.* **2009**, *131*, 4788.
(24) Wu, D. G.; Cahen, D.; Graf, P.; Naaman, R.; Nitzan, A.; Shvarts, D. *Chem.—Eur. J.* **2001**, *7*, 1743.
(25) Bruening, M.; Moons, E.; Cahen, D.; Shanzer, A. *J. Phys. Chem.* **1995**, *99*, 8368.
(26) Bastide, S.; Butruille, R.; Cahen, D.; Dutta, A.; Libman, J.; Shanzer, A.; Sun, L.; Vilan, A. *J. Phys. Chem. B* **1997**, *101*, 2678.
(27) Cohen, R.; Kronik, L.; Vilan, A.; Shanzer, A.; Cahen, D. *Adv. Mater.* **2000**, *12*, 33.
(28) Bent, S. F.; Kachian, J. S.; Rodríguez-Reyes, J. C. F.; Teplyakov, A. V. *Proc. Natl. Acad. Sci. U.S.A.* **2011**, *108*, 956.
(29) Yaffe, O.; Scheres, L.; Puniredd, S. R.; Stein, N.; Biller, A.; Lavan, R. H.; Shpaisman, H.; Zuilhof, H.; Haick, H.; Cahen, D.; Vilan, A. *Nano Lett.* **2009**, *9*, 2390.
(30) Cass, A. E. G. *Electron. Lett.* **2007**, *43*, 903.
(31) Waleed, S. M.; Jamal, D. M.; Starikov, E. B.; Cuniberti, G. *Adv. Funct. Mater.* **2010**, *20*, 1865.
(32) Della, P. E. A.; MacDonald, J. E.; Elliott, M.; Jones, D. D. *Small* **2012**, *8*, 2341.
(33) Katz, E.; Willner, I. *Electroanalysis* **2003**, *15*, 913.
(34) Grieshaber, D.; MacKenzie, R.; Voros, J.; Reimhult, E. *Sensors* **2008**, *8*, 1400.
(35) Stern, E.; Vacic, A.; Reed, M. A. *IEEE Trans. Electron Devices* **2008**, *55*, 3119.
(36) Haruyama, T. *Mater. Technol. (London, U.K.)* **2011**, *26*, 163.

(37) Rusmini, F.; Zhong, Z.; Feijen, J. *Biomacromolecules* **2007**, *8*, 1775.
(38) Jonkheijm, P.; Weinrich, D.; Schroeder, H.; Niemeyer, C. M.; Waldmann, H. *Angew. Chem., Int. Ed.* **2008**, *47*, 9618.
(39) Whaley, S. R.; English, D. S.; Hu, E. L.; Barbara, P. F.; Belcher, A. M. *Nature* **2000**, *405*, 665.
(40) Sarikaya, M.; Tamerler, C.; Jen, A. K. Y.; Schulten, K.; Baneyx, F. *Nat. Mater.* **2003**, *2*, 577.
(41) Tamerler, C.; Khatayevich, D.; Gungormus, M.; Kacar, T.; Oren, E. E.; Hnilova, M.; Sarikaya, M. *Pept. Sci.* **2010**, *94*, 78.
(42) Galloway, J. M.; Staniland, S. S. *J. Mater. Chem.* **2012**, *22*, 12423.
(43) Tamerler, C.; Sarikaya, M. *ACS Nano* **2009**, *3*, 1606.
(44) Sanghvi, A. B.; Miller, K. P. H.; Belcher, A. M.; Schmidt, C. E. *Nat. Mater.* **2005**, *4*, 496.
(45) Matmor, M.; Ashkenasy, N. *J. Mater. Chem.* **2011**, *21*, 968.
(46) Pender, M. J.; Sowards, L. A.; Hartgerink, J. D.; Stone, M. O.; Naik, R. R. *Nano Lett.* **2005**, *6*, 40.
(47) Nochomovitz, R.; Amit, M.; Matmor, M.; Ashkenasy, N. *Nanotechnology* **2010**, *21*, 145305.
(48) Dezieck, A.; Acton, O.; Leong, K.; Oren, E. E.; Ma, H.; Tamerler, C.; Sarikaya, M.; Jen, A. K. Y. *Appl. Phys. Lett.* **2010**, *97*, 013307.
(49) Kronik, L.; Shapira, Y. *Surf. Sci. Rep.* **1999**, *37*, 1.
(50) Aphek, O. B.; Kronik, L.; Leibovitch, M.; Shapira, Y. *Surf. Sci.* **1998**, *409*, 485.
(51) Spicer, W. E.; Eglash, S.; Lindau, I.; Su, C. Y.; Skeath, P. R. *Thin Solid Films* **1982**, *89*, 447.
(52) Harriman, A. *J. Phys. Chem.* **1987**, *91*, 6102.
(53) Grätzel, M. *Nature* **2001**, *414*, 338.
(54) Goede, K.; Busch, P.; Grundmann, M. *Nano Lett.* **2004**, *4*, 2115.
(55) Goede, K.; Grundmann, M.; Holland-Nell, K.; Beck-Sickinger, A. G. *Langmuir* **2006**, *22*, 8104.
(56) Willett, R. L.; Baldwin, K. W.; West, K. W.; Pfeiffer, L. N. *Proc. Natl. Acad. Sci. U.S.A.* **2005**, *102*, 7817.
(57) Peelle, B. R.; Krauland, E. M.; Wittrup, K. D.; Belcher, A. M. *Langmuir* **2005**, *21*, 6929.
(58) Vallee, A.; Humblot, V.; Pradier, C. M. *Acc. Chem. Res.* **2010**, *43*, 1297.